

Article

Expression, Purification and Characterization of C-FADD

Yuan Chen¹, Dingyuan Ma¹, Qi-Lai Huang¹, Weijuan Zheng¹, Jing Zhang¹, Yi Shen¹, Jiahuang Li¹, Wei Dong¹, Min Lu¹, Jin Wang¹ and Zi-Chun Hua^{1,2,3}

FADD is an important proapoptotic adaptor in death receptor-induced apoptosis. Recently, FADD has been found to participate in a variety of non-apoptotic processes, such as development, cell cycle progression and survival. Its non-apoptotic activities were regulated by the phosphorylated status of the serine residue located at the C-terminal region, a domain distinct from the proapoptotic function related DED and DD domains. However, due to the difficulties in expression and crystallization of natural FADD, by far the molecular structures of all FADD variants did not contain the C-terminal region. To elucidate the structure-function relationship of C-terminal region, we need to obtain an FADD variant that containing C-terminal region. In this study, mouse FADD (80-205) containing DD domain and C-terminal region, designated as C-FADD, was expressed in *E. coli* with His-tag at the N-terminus and purified by Ni²⁺ affinity chromatography. The purified protein existed as a homogenous monomer in glutaraldehyde cross-linking analysis and exhibited a typical α -helix spectrum in CD (circular dichroism) assay. *In vitro* His-tag pull-down assay demonstrated that the purified C-FADD possessed the CK I α -binding activity which was important for its non-apoptotic function. *Cellular & Molecular Immunology*. 2009;6(4):295-301.

Key Words: C-FADD, expression, purification, monomer

Introduction

The Fas-associated death domain (FADD), as a cytosolic adaptor protein, plays a significant role in death receptor (DR)-mediated cell death. In FADD gene knockout mice (1, 2), cells were protected against apoptosis induced by activated Fas. Murine FADD is composed of 205 amino acid residues, and contains two distinct functional domains with similar structure, an N-terminal death effector domain (DED) and a C-terminal death domain (DD). In addition, its C-terminus has been proposed as a putative third-functional domain, C-terminal domain (CTD), which contains an important single phosphorylation site in a serine-rich region (3, 4).

Homotypic interactions between DDs or DEDs were

proposed to be very important in apoptosis signaling pathways. FADD was first identified by yeast two-hybrid screen using the intracellular death domain of Fas/APO1/CD95 as a bait (5-7). Upon activation by Fas ligand (Fas L), Fas binded to FADD through DD-DD interaction, and then the DED of FADD associated with the DED of tandem DED-containing initiator procaspase-8 to form the death-inducing signaling complex (DISC). When approximated, the procaspase-8 was activated by self-cleavage, and then activated downstream effector caspases, which triggered various apoptotic processes (8). In addition to Fas, FADD also could directly or indirectly interact with other death receptors such as TNFR 1, DR 3, DR 4 and DR 5 (9), to transduce signals from activated DRs. FLIPs were also capable to bind to FADD or caspase-8 *via* DED-DED interaction to regulate the apoptosis by interfering with the caspase-8 activation (10).

Recently, many reports disclosed the participation of FADD in a variety of non-apoptotic processes, including innate immune signaling, embryogenesis, hematopoiesis, lymphocyte cell cycle progression and survival (11). Mice with germline ablation of FADD died in utero at around 10 d during embryonic gestation, which contrasted with the viability of Fas- and TNFR 1-deficient animals (2). Characterizations of FADD^{-/-} or FADD-DN-expressing T cells showed that proliferation and development after activation were impaired (12) and progresses in cell cycle were blocked (13, 14). The mechanistic basis for these non-apoptotic activities was presently unclear, just indicating that the function might depend on the phosphorylation of the

¹The State Key Laboratory of Pharmaceutical Biotechnology and Jiangsu Center of Hepatobiliary Diseases, College of Life Sciences, Nanjing University, Nanjing 210093, China;

²Changzhou High-Tech Research Institute of Nanjing University, Changzhou 213164, China;

³Correspondence to: Dr. Zi-Chun Hua, the State Key Laboratory of Pharmaceutical Biotechnology and Jiangsu Center of Hepatobiliary Diseases, College of Life Sciences, Nanjing University, Nanjing 210093, China. Tel: +86-25-8332-4605, Fax: +86-25-8332-4605, E-mail: zchua@nju.edu.cn

Received Aug 2, 2009. Accepted Aug 18, 2009.

©2009 Chinese Society of Immunology and University of Science & Technology of China

third functional region at the C-terminus (CTD) (15). The Ser194 in human FADD (3, 14), equivalent to Ser191 in mouse FADD (16), was the exclusive phosphorylated site, significant for regulation of cell growth, proliferation and cell cycle. FADD was highly phosphorylated in cells arrested in G2/M, while phosphorylation was low in G1/S. However, the phosphorylation state had no contribution to apoptosis.

C-FADD (C-terminal half of FADD which lacks the death effector domain) (17), which was also called FADD-DN (a dominant negative mutant of FADD lacking the N-terminal death effector domain), displayed apoptosis inhibition activity on C-FADD overexpression-transgenic mice model (17, 18). Furthermore, C-FADD-transgenic mice had both impaired apoptosis and T cell proliferation (19). C-FADD blocked those TNF receptor family members that used FADD as an adapter. C-FADD expression enhanced deletion of autoreactive thymocytes and inhibited proliferation of mature T lymphocytes, blocking both quiescent cells from entering the cell cycle (the G0/S transition) and the proliferation of continuously cycling T cells in G1 (19). Furthermore, it was observed that C-FADD exerted a similar growth-inhibitory effect on fibroblasts, indicating that this effect was not limited to T cells and was likely to act on more general, cell type-independent proliferation pathway (20). The above observations strongly suggested that C-FADD had a conformation identical or highly similar to the full length FADD so that it could effectively interfere or compete with the both apoptotic and non-apoptotic functions of FADD. We attribute the dominant negative function in both apoptotic and non-apoptotic pathways of C-FADD to the retaining of its C-terminal domain which contains the major phosphorylation site of FADD.

Despite of the pivotal role of the C-terminal region, little is known about its structure. The individual three-dimensional structure of hFADD-DED (residues 1-83), mFADD-DD (residues 89-183), hFADD-DD (residues 93-192) and hFADD (residues 1-191) in solution were well resolved by NMR (21-24), none of which contained the third functional domain involved in non-apoptotic processes.

In the present study, mouse C-FADD, mFADD (80-205) containing the DD domain and C-terminal region, was expressed and purified from *E. coli* with the fusion of His₆-tag at the N-terminus. The purified recombinant protein was shown to be a monomer with good homogeneity and possess the folding fashion similar to FADD DD domain. As expected, it remained the intrinsic CK I α -binding activity.

Materials and Methods

Construction of His₆-C-FADD expressing plasmid

The ORF encoding mouse FADD (80-205) was amplified by PCR with primers containing Nde I and Hind III site (underlined) respectively (upstream primer: 5'- ggaattc cat atg gac gac ttc gag gcg g -3'; downstream primer: 5'- cgcg aagctt tca ggg tgt ttc tga gg -3'). The PCR product was digested by Nde I and Hind III, and then inserted into the vector pET28a (Novagen, USA) to generate N-terminal

His-tagged His₆-C-FADD (mFADD_{80-205aa}) expressing plasmid (pET28a-His₆-C-FADD).

Expression of recombinant His₆-C-FADD

The recombinant plasmid was transformed into *E. coli* BL21 (DE3) cells (Novagen). 10 mL culture from a single colony was grown at 37°C overnight and inoculated into 1 L fresh LB medium, and then grown at 25°C. When the culture reached the mid-log phase (optical density at 600 nm around 0.8-1.0), IPTG was added to a final concentration of 0.4 mM to induce the expression of target protein. After additional 5 h cultivation at 25°C, the cells were harvested by centrifugation at 8000 rpm for 6 min and resuspended in 40 mL lysis buffer (150 mM NaCl, 10% glycerol, 1 mM PMSF, 20 mM Tris-HCl, pH 8.0). After sonication disruption, cell lysates were separated into soluble proteins and insoluble cell debris by centrifugation at 15,000 g for 30 min at 4°C. The soluble supernatant was applied for purification.

Purification of His-tagged fusion protein

His-tagged fusion proteins were generally purified by two tandem chromatography: immobilized metal affinity chromatography on a nickel column and size exclusion chromatography on a Sephadex G-15 column.

The clarified cell lysate supernatant was loaded onto a Ni²⁺ affinity column pre-equilibrated with 20 mM Tris-HCl, pH 8.0, containing 20 mM imidazole and 150 mM NaCl. After OD280 was washed to baseline with the same buffer, proteins were eluted by buffers with increasing concentration of imidazole. Nonspecific binding proteins and His-tagged proteins were eluted sequentially. The elution fraction containing target protein was loaded onto a Sephadex G-15 column using the buffer of 20 mM Tris-HCl, pH 8.0, to get rid of imidazole and NaCl in the sample. Protein concentration was determined by Bradford assay using bovine serum albumin as a standard.

Polyacrylamide gel electrophoresis analysis

Fractions from each chromatography step were analyzed by reducing SDS-PAGE and stained with Coomassie blue R-250 as conventional procedures. Gels were scanned using UVP white/ultraviolet transilluminator and quantitative analysis was performed using Grab-it 2.5 and Gelwork software. Continuous non-denaturing PAGE was carried out similarly to SDS-PAGE, except for the absence of SDS and reducing agents in the system.

Cross-linking experiments

Protein samples were cross-linked with glutaraldehyde as described by Monteiro et al (25). Briefly, 75 μ L of 120 μ g/mL solution of each interest protein was incubated with 0.1% glutaraldehyde (v/v) at room temperature for 20 min. Then reactions were stopped by adding SDS sample buffer and the cross-linked products were directly resolved by SDS-PAGE.

Analytical size exclusion chromatography

Approximately 500 μ L (about 200 μ g) isolated recombinant

protein was loaded onto a Sephacryl S-200 HR 16/60 column (Pharmacia) pre-equilibrated with buffer A (20 mM Tris-HCl, pH 8.0, 150 mM NaCl) using a manual injector (0.5 μ L loop). Chromatography was performed on an AKTA FPLC system at a flow rate of 0.8 ml/min at room temperature and the absorbance was monitored at 280 nm. BSA (bovine serum albumin, 66.2 kDa) and ZZ (22 kDa) (26) proteins were used as standard molecular weight markers under the same conditions to calibrate the column.

Circular dichroism spectroscopy

Circular dichroism (CD) in far-UV measurement was made in a Jasco J-810 spectropolarimeter in quartz cell of 1 mm pathlength at room temperature, using the following parameters: 1-s response, 50 nm/min scan speed, 0.1 nm data acquisition interval, 3 accumulations, 2-nm bandwidth. The spectra were recorded over the range of 190–250 nm at a protein concentration of 0.2 mg/mL in buffer containing 20 mM Tris-HCl, pH 8.0, and baseline-corrected by subtraction of blank buffer. Ellipticity was reported as molar ellipticity $[\theta]$ (mdeg.cm².mol⁻¹).

Fluorescence spectroscopy

Fluorescence emission spectra were recorded from 300 to 400 nm on an Aminco SPF-500 spectrofluorimeter using a protein concentration of 50 μ g/ μ L in 20 mM Tris-HCl, pH 8.0. Samples were excited at 280 nm with a semimicro 1 cm light path cell. The excitation and emission spectral bandwidths were both 3 nm.

Cell culture and transfection

Human embryonic kidney SV40 large T-antigen expressing (TSA) cells (293T) were cultured in Dulbecco's modified Eagle medium (DMEM, Gibco, USA) at 37°C in a humidified atmosphere of 95% air and 5% CO₂, supplemented with 10% new born calf serum, 100 units/mL penicillin, 100 μ g/ml streptomycin. For transfection, 5×10^5 cells were seeded in a 60-mm culture dish. Confluent cells (80%) were then transfected with 5 μ g FLAG-CK I α -expressing plasmid with M-PEI as described (27). Two days later, harvested cells were washed with cold phosphate-buffered saline (PBS) and lysed at 4°C in lysis buffer (20 mM Tris-HCl, pH 8.0, 150 mM NaCl, 10% glycerol, 1% Triton X-100 plus complete protease inhibitor cocktail (Roche, USA)) followed by centrifugation at 14,000 rpm for 15 min to remove insoluble material.

His-tag pull-down assay

Before pull-down, His-tagged fusion protein-immobilized sepharose beads were prepared. Briefly, 150 μ g purified His-tagged C-FADD or control protein (GST) were respectively mixed with 5 μ L Ni-metal chelating affinity resin in binding buffer (20 mM Tris-HCl, pH 8.0, 150 mM NaCl, 10% glycerol, 1 mM PMSF) by rotating at 4°C for 4 h. By centrifugation at 800 g for 3 min, the supernatant was removed. Then the beads were washed four times with wash buffer (20 mM Tris-HCl, pH 8.0, 1 M NaCl, 10% glycerol, 0.1% Triton X-100, 1 mM PMSF). For each time, the beads

were incubated with the wash buffer on a rotator for 10 min and collected by centrifugation. After extensively rinse, the beads were mixed with equal amount of soluble FLAG-CK I α -overexpressing cell lysates (500 μ g) by incubation for 4 h at 4°C on the rotator. The beads were washed five times again with the same wash buffer, boiled in SDS sample loading buffer for 5 min and resolved by SDS-PAGE for immunoblotting detecting or Coomassie blue staining.

Western blot analysis

After SDS-PAGE, proteins were transferred to 0.45 μ m PVDF membranes (Pall Corporation, USA). After 1 h of blocking with 5% non-fat milk in PBST (PBS, 0.05% Tween-20), the membrane was incubated with the appropriate specific antibody (anti-Flag) in PBST with 5% milk for 1 h. Then the membrane was washed four times in PBST for 5 min. Afterwards, HRP conjugated goat anti-mouse IgG antibody (Santa Cruz Biotechnology, USA), which had been diluted 2000-fold in PBST with 5% milk, was added for another 1 h of incubation. After three 10-min washes with PBST, the signal was developed with enhanced chemiluminescence (ECL) detection system (Cell Signaling, USA) followed by exposure to X-ray film.

Results

Expression and purification of His-tagged C-FADD

mFADD(80–205) was expressed with a His₆-tag fused at the N-terminus, which facilitated the purification while didn't interfere with the C-terminus. The recombinant protein C-FADD had 147 amino acid residues, including the DD domain, the C-terminal domain and the residual amino acids from the vector pET28a at the N-terminus. As shown in SDS-PAGE analysis (Figure 1), after IPTG induction, the protein was expressed at the expected molecular weight (16.1 kDa) in *E. coli*. It accounted for about 26% of the total cellular proteins. After sonication and centrifugation, almost

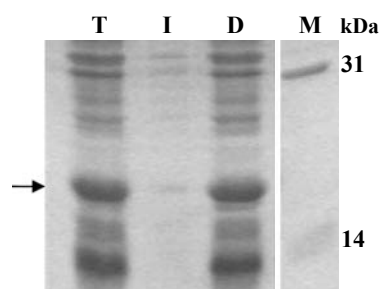


Figure 1. SDS-PAGE analysis of C-FADD expressed in *E. coli*. After 5 h induction at 25°C, cells were collected for sonication. By centrifugation, total proteins (T) were separated into soluble (S) and insoluble (I) fractions. The insoluble fraction was re-suspended in a volume equal to that of the soluble fraction. Protein size markers (M) are indicated in kDa. Arrowhead indicates the induced target protein C-FADD.

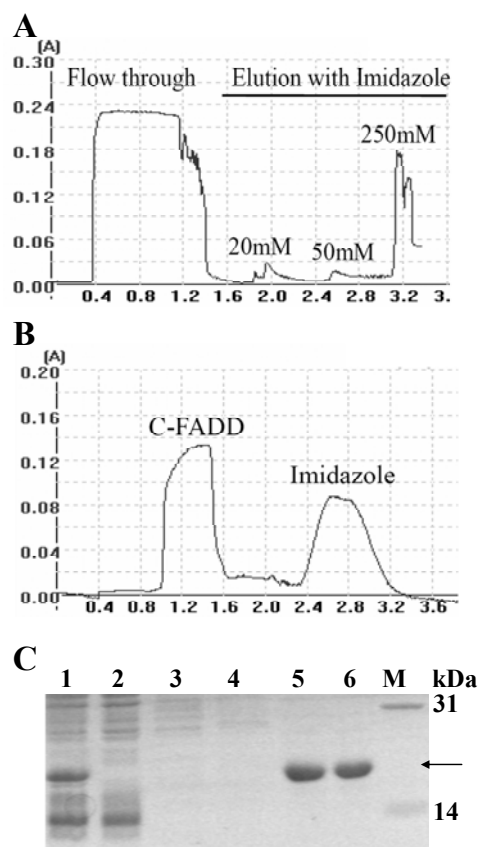


Figure 2. Chromatographic profiles and SDS-PAGE analysis of C-FADD purification. C-FADD-expression supernatant was first purified *via* Ni-chelated affinity chromatography (A) and then the elution fraction with 250 mM imidazole was further purified *via* a Sephadex G15 column to remove imidazole (B). The samples were analyzed by SDS-PAGE and Coomassie Brilliant Blue R250 staining (C). Lane 1, supernatant of C-FADD-expressing BL21 (DE3) after sonication and centrifugation; Lane 2, flow-through of Ni^{2+} -sepharose column chromatography; Lanes 3-5, fractions eluted by 20 mM, 50 mM, and 250 mM imidazole respectively; Lane 6, C-FADD-containing flow-through from G15; Lane M, molecular weight marker. The arrow indicates the band of C-FADD.

all the expressed target protein was released into the soluble fraction with a natively folded conformation.

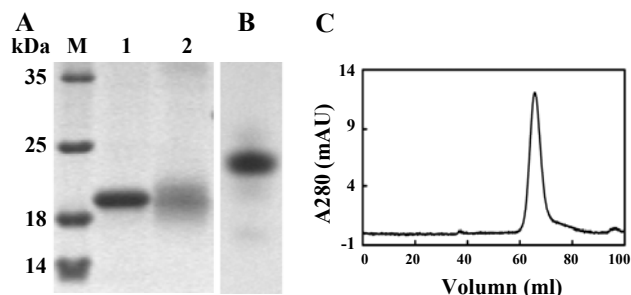


Figure 3. Characterization of the purified recombinant C-FADD. (A) Glutaraldehyde cross-linking assay. The reaction was performed 20 min at room temperature in the absence (Lane 1) or presence (Lane 2) of 0.1% glutaraldehyde. Then the products were resolved by 12% SDS-PAGE. (B) Non-reducing-native PAGE (6%) analysis of C-FADD. (C) Size exclusion chromatography profile of C-FADD. Sample (500 μl) was loaded on a Sephacryl S-200 HR 16/60 column equilibrated with 20 mM Tris-HCl, pH 8.0, 150 mM NaCl, at a rate of 0.8 ml/min.

The soluble recombinant protein was then purified by affinity chromatography on a Ni-chelated agarose column (Figure 2A). SDS-PAGE analysis showed that His-tagged C-FADD exhibited high-affinity for Ni^{2+} column (Figure 2C). No target protein was detected in the flow-through of the nickel affinity column, and the tight binding could not be disrupted by low concentrations of imidazole, until elution with 250 mM imidazole. This resulted in the high purity of target protein. Since high concentration of imidazole is harmful to long-term storage of protein, it has to be removed from the purified protein. Making use of the difference in molecular size between C-FADD and imidazole, imidazole was got rid of successfully by gel chromatography on a Sephadex G-15 column. Two separated elution peaks representing the purified protein C-FADD and imidazole respectively were observed in the chromatographic profile in Figure 2B.

As a result, about 42 mg recombinant C-FADD was recovered from 1 liter of bacteria culture. A summary of the purification steps and protein yield is presented in Table 1.

Characterization of purified C-FADD

As glutaraldehyde can freeze the association state quickly, a

Table 1. Purification of C-FADD from *E. coli* extract (1 liter of fermentation)^a

Purification step	Total protein (mg) ^b	Purity (%) ^c	C-FADD (mg) ^d	Stepwise recovery (%)	Final yield (%)
supernatant	300	26	78	100	
Ni^{2+} affinity chromatography	56	90	50.4	64.6	
Gel filtration	46	91	41.9	83.1	15.3

^aData are normalized to quantities obtained per liter growth medium;

^bQuantitated by Bradford method;

^cQuantitated by densitometric scanning of the SDS-PAGE gel;

^dThe amount of C-FADD protein is calculated as: the input total protein \times the purity of C-FADD in each step.

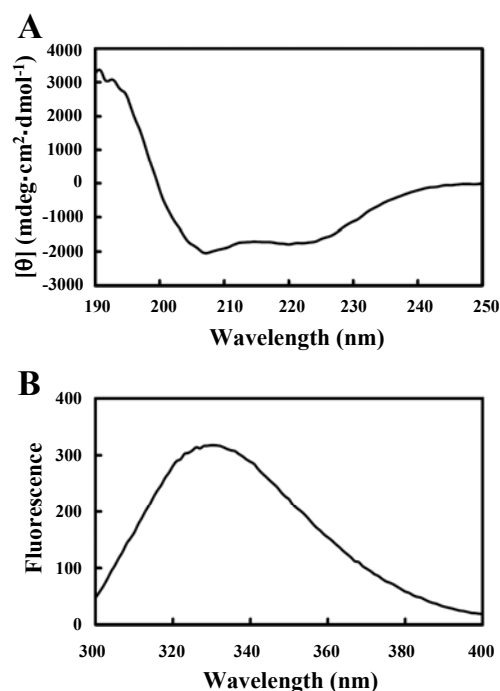


Figure 4. Spectroscopic studies of C-FADD. (A) Far-UV CD spectrum of C-FADD. (B) The intrinsic fluorescent spectrum of C-FADD excited at 280 nm.

cross-linking experiment was performed to detect the aggregation state of C-FADD. Reducing SDS-PAGE can disrupt the association of proteins completely, only if they are cross-linked by glutaraldehyde. On SDS-PAGE gel, the product of glutaraldehyde cross-linking had the same mobility as that in the absence of glutaraldehyde (Figure 3A). It suggested that C-FADD existed as a monomer in natural state. Under the condition of SDS-PAGE, not only the association among subunits was interrupted but also the interactions within the subunit were broken. In order to examine the homogeneity of the molecular structure under natural condition, native PAGE without SDS and reducing reagent was carried out. C-FADD also exhibited as a single band (Figure 3B).

The results indicated that the monomeric C-FADD protein possessed pretty good homogeneity. The monomeric state, high purity and good homogeneity of the purified recombinant C-FADD were further confirmed by size exclusion chromatography. Only a single major chromatographic peak was detected for C-FADD, the retention volume of which was 65.7 ml. Compared with the 64.6 ml of retention volume for ZZ protein, which is a 22 kDa synthetic Fc region-binding domain purified in our lab (26), the elution volume of 65.7 ml for C-FADD indicated its molecular weight was smaller than 22 kDa. It further confirmed that C-FADD existed as a monomer form. All of the characterization made the protein suitable for a further study on structure.

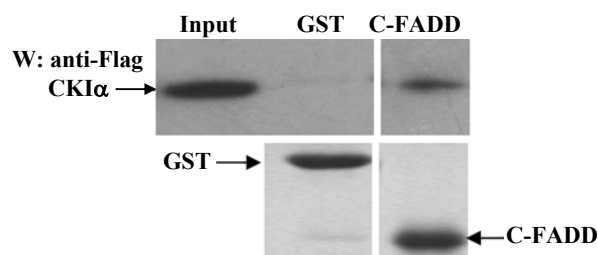


Figure 5. Protein-protein interaction investigation *in vitro* by His pull-down assay. His-tagged C-FADD or GST (control) coupled Ni^{2+} resins were incubated with lysates of 293T cells overexpressing Flag-CK I α . Proteins bound to the beads and 10% of the input lysate were immunoblotted with Flag antibody (upper panel). Meanwhile, a portion of the recovered proteins were separated on gels, and subjected to Coomassie blue staining to ensure equal loading of His-tagged proteins (lower panel).

Secondary structure analysis by spectroscopy

Far-UV CD spectrum can be used empirically as “fingerprints” of a particular protein, providing information about the polypeptide backbone and the protein conformation in terms of its secondary structure (28). As depicted in Figure 4A, C-FADD had two negative peaks around 222 nm and 208 nm and a stronger positive peak near 190 nm, which was a characteristic α -helix protein spectrum. It was consistent with the previous reports of the three-dimensional solution structure of CTD-deficient FADD derivative proteins (21–22, 24). At the same time, the intrinsic fluorescence of C-FADD was also studied to disclose the microenvironment surrounding the residues of tyrosine and tryptophan which located at the DD domain. When excited at 280 nm, the maximum emission of C-FADD was recorded at 333 nm. It meant that Trp and Tyr residues were mainly located in nonpolar environment. Therefore the addition of His-tag and the C-terminal fragment to the both two terminus of FADD DD domain as designed did not affect the folding of DD domain.

CK I α -binding capability of C-FADD

Purified recombinant protein C-FADD was used in protein-protein interaction assay through His pull-down experiment to determine whether it could bind to CK I α , a analogue of the full-length FADD as reported (29). The specificity of the experiment would be proven with His-GST as control. The Coomassie blue staining result (Figure 5 the lower panel) showed that almost equivalent His-tag proteins (His-GST and His-C-FADD) were immobilized on the beads. For the control group (GST protein), no CK I α was detected in his-tag pull-down assay (Figure 5 the upper panel), indicating that CK I α did not have non-specific binding to either Ni-metal chelating affinity resin or His-tagged GST protein. For the C-FADD group, CK I α was detected, indicating that C-FADD could bind to CK I α (Figure 5 the upper panel) and DED domain was not a prerequisite for CK I α binding and phosphorylation.

Discussion

The delineations of DED and DD structures helped us understand the actions of FADD in the apoptosis signaling pathway more deeply. With the discovery of non-apoptotic function of FADD, more and more studies were performed to underline the role of the C-terminal region involved in the non-apoptosis process. However, up to now, there is no structural analysis focused on the third functional domain. The aim of our present study is to express and purify the C-terminal region-containing FADD for further research. Due to the difficulty in the expression and purification of the whole FADD molecule and its instability, no full-length FADD could be obtained to qualify for structural determination (23). In the present paper, the DED domain, which was supposed to mediate FADD self-association, was deleted from mFADD (30, 31). The recombinant mFADD contains DD domain and CTD domain.

His₆-tag was fused to the N-terminal of mFADD (80-205), which avoided interference between the tag and the C-terminal functional region. The recombinant protein C-FADD was well induced in *E. coli* BL21 (DE3) with high solubility and showed high affinity for nickel resin. It suggested that the His-tag was exposed outside the protein surface. As a result, the protein was easily purified with high purity. Consistent with the previous studies (30, 31), the DED-deficient C-FADD existed as a monomer. This result further supports the notion that FADD usually exists in monomer form, and only upon apoptotic stimulation, it participates in the formation of DISC (the death-inducing signaling complex) in trimer form *via* interacting with TNFR by DD domain and associating with procaspase-8 by DED domain.

The purified C-FADD protein had good homogeneity and was suitable for further structural studies. C-FADD also exhibited characteristic folding mode mainly consisting of α -helices similar to the DD structure (21, 24), indicating that the C-terminal region does not affect the secondary structure of DD domain. Consistent with the result, the mutation at the FADD phosphorylation site Ser191 was reported not to affect its ability to transmit death receptor-induced apoptotic signals in normal cells (16).

On the contrary, the FADD phosphorylation state at the C-terminal was found to correlate with its non-apoptotic activity. To investigate the biological function of phosphorylated FADD protein, the phosphorylation site of FADD, Ser 191, was mutated to Asp (FADD (S191D)) and the aim of this mutation was to mimic constitutively phosphorylated Ser 191 (16). In transgenic mice expressing FADD (S191D), T cells were defective in cell cycle progression. And with age, FADD (S191D) mice became runted and anemic and exhibited splenomegaly (16). In phase G2/M, Ser194 in hFADD, equivalent to Ser191 in mFADD, can bind with and be phosphorylated by its kinase CK I α to regulate the G2/M transition (3, 29). As for the mechanism underlying how the FADD phosphorylation status regulates its function in cell survival and cell cycle progression, little is

known. Our results clearly demonstrated that interaction between FADD and its kinase CK I α was DED domain-independent, but resulted from FADD phosphorylation. This phenomenon is consistent with the previous reports that C-FADD-transgenic mice displayed non-apoptotic function blockage phenotype (19). Based on the previous data, we hypothesize that the C-terminal region is probably in a conformation of high flexibility without fixed folding conformation. When phosphorylated, the flexibility conformation may change, resulting in the binding affinity to an unknown protein. To prove the hypothesis, more detailed studies need to be performed. The production of large amounts of soluble C-FADD will allow us to purify enough protein to carry out structural and functional analysis and elucidate the molecular basis of FADD apoptotic and non-apoptotic functions.

Acknowledgements

The authors are grateful to grants from the Chinese National Nature Sciences Foundation (30425009, 30330530, 30730030, 30600320, 30821006) and Jiangsu Provincial Department of Health.

References

1. Zhang JK, Cado D, Chen A, Kabra NH, Winoto A. Fas-mediated apoptosis and activation-induced T-cell proliferation are defective in mice lacking FADD/Mort1. *Nature*. 1998;392:296-300.
2. Yeh WC, de la Pompa JL, McCurrach ME, et al. FADD: Essential for embryo development and signaling from some, but not all, inducers of apoptosis. *Science*. 1998;279:954-1958.
3. Scaffidi C, Volkland J, Blomberg I, Hoffmann I, Krammer PH, Peter ME. Phosphorylation of FADD/MORT1 at serine 194 and association with a 70-kDa cell cycle-regulated protein kinase. *J Immunol*. 2000;164:1236-1242.
4. Barnhart BC, Lee JC, Alappat EC, Peter ME. The death effector domain protein family. *Oncogene*. 2003;22:8634-8644.
5. Zhang J, Winoto A. A mouse Fas-associated protein with homology to the human Mort1/FADD protein is essential for Fas-induced apoptosis. *Mol Cell Biol*. 1996;16:2756-2763.
6. Boldin MP, Varfolomeev EE, Pancer Z, Mett IL, Camonis JH, Wallach D. A novel protein that interacts with the death domain of Fas/APO1 contains a sequence motif related to the death domain. *J Biol Chem*. 1995;270:7795-7798.
7. Chinnaiyan AM, O'Rourke K, Tewari M, Dixit VM. FADD, a novel death domain-containing protein, interacts with the death domain of Fas and initiates apoptosis. *Cell*. 1995;81:505-512.
8. Peter ME, Krammer PH. The CD95 (APO-1/Fas) DISC and beyond. *Cell Death Differ*. 2003;10:26-35.
9. Ashkenazi A, Dixit VM. Death receptors: Signaling and modulation. *Science*. 1998;281:1305-1308.
10. Krueger A, Baumann S, Krammer PH, Kirchhoff S. FLICE-inhibitory proteins: Regulators of death receptor-mediated apoptosis. *Mol Cell Biol*. 2001;21:8247-8254.
11. Werner MH, Wu CW, Walsh CM. Emerging roles for the death adaptor FADD in death receptor avidity and cell cycle regulation. *Cell Cycle*. 2006;5:2332-2338.
12. Walsh CM, Wen BG, Chinnaiyan AM, O'Rourke K, Dixit VM,

- Hedrick SM. A role for FADD in T cell activation and development. *Immunity*. 1998;8:439-449.
13. Kabra NH, Kang CH, Hsing LC, Zhang JK, Winoto A. T cell-specific FADD-deficient mice: FADD is required for early T cell development. *Proc Natl Acad Sci U S A*. 2001;98:6307-6312.
14. Alappat EC, Volkland J, Peter ME. Cell cycle effects by C-FADD depend on its C-terminal phosphorylation site. *J Biol Chem*. 2003;278:41585-41588.
15. Zhang J, Zhang DP, Hua ZC. FADD and its phosphorylation. *IUBMB Life*. 2004;56:395-401.
16. Hua ZC, Sohn SJ, Kang C, Cado D, Winoto A. A function of Fas-associated death domain protein in cell cycle progression localized to a single amino acid at its C-terminal region. *Immunity*. 2003;18:513-521.
17. Chinnaiyan AM, Tepper CG, Seldin MF, et al. FADD/MORT1 is a common mediator of CD95 (Fas/APO-1) and tumor necrosis factor receptor-induced apoptosis. *J Biol Chem*. 1996;271:4961-4965.
18. Chinnaiyan AM, O'Rourke K, Yu GL, et al. Signal transduction by DR3, a death domain-containing receptor related to TNFR-1 and CD95. *Science*. 1996;274:990-992.
19. Newton K, Harris AW, Bath ML, Smith KG, Strasser A. A dominant interfering mutant of FADD/MORT1 enhances deletion of autoreactive thymocytes and inhibits proliferation of mature T lymphocytes. *EMBO J*. 1998;17:706-718.
20. Hueber AO, Zornig M, Bernard AM, Chautan M, Evan G. A dominant negative Fas-associated death domain protein mutant inhibits proliferation and leads to impaired calcium mobilization in both T-cells and fibroblasts. *J Biol Chem*. 2000;275:10453-10462.
21. Berglund H, Olerenshaw D, Sankar A, Federwisch M, McDonald NQ, Driscoll PC. The three-dimensional solution structure and dynamic properties of the human FADD death domain. *J Mol Biol*. 2000;302:171-188.
22. Carrington PE, Sandu C, Wei Y, et al. The structure of FADD and its mode of interaction with procaspase-8. *Mol Cell*. 2006;22:599-610.
23. Eberstadt M, Huang B, Chen Z, et al. NMR structure and mutagenesis of the FADD (Mort1) death-effector domain. *Nature*. 1998;392:941-945.
24. Jeong EJ, Bang S, Lee TH, Park YI, Sim WS, Kim KS. The solution structure of FADD death domain. Structural basis of death domain interactions of Fas and FADD. *J Biol Chem*. 1999;274:16337-16342.
25. Monteiro KM, Scapin SMN, Navarro MVAS, et al. Self-assembly and structural characterization of Echinococcus granulosus antigen B recombinant subunit oligomers. *Biochim Biophys Acta-Proteins and Proteomics*. 2007;1774:278-285.
26. Chen C, Huang QL, Jiang SH, Pan X, Hua ZC. Immobilized protein ZZ, an affinity tool for immunoglobulin isolation and immunological experimentation. *Biotechnol Appl Biochem*. 2006;45:87-92.
27. Li SF, Dong W, Zong YW, et al. Polyethylenimine-complexed plasmid particles targeting focal adhesion kinase function as melanoma tumor therapeutics. *Mol Ther*. 2007;15:515-523.
28. Pain R. Determining the CD spectrum of a protein. In: *Current Protocols in Protein Science*. John Wiley & Sons, Inc; 1996;7:1-23.
29. Alappat EC, Feig C, Boyerinas B, et al. Phosphorylation of FADD at serine 194 by CKI alpha regulates its nonapoptotic activities. *Mol Cell*. 2005;19:321-332.
30. Muppidi JR, Lobito AA, Ramaswamy M, Yang JK, Wang L, Wu H, Siegel RM. Homotypic FADD interactions through a conserved RXDLL motif are required for death receptor-induced apoptosis. *Cell Death Differ*. 2006;13:1641-1650.
31. Sandu C, Morisawa G, Wegorzewska I, et al. FADD self-association is required for stable interaction with an activated death receptor. *Cell Death Differ*. 2006;13:2052-2061.